PUBLISHED VERSION

Warren-Smith, Stephen; Afshar Vahid, Shahraam; Monro, Tanya Mary.
Fluorescence-based sensing with optical nanowires: a generalized model and experimental validation, *Optics Express*, 2010; 18(9):9474-9485.

Copyright © 2010 Optical Society of America

PERMISSIONS

http://www.opticsinfobase.org/submit/review/copyright_permissions.cfm#posting

This paper was published in Optics Express and is made available as an electronic reprint with the permission of OSA. The paper can be found at the following URL on the OSA website http://www.opticsinfobase.org/abstract.cfm?URI=oe-18-9-9474. Systematic or multiple reproduction or distribution to multiple locations via electronic or other means is prohibited and is subject to penalties under law.

OSA grants to the Author(s) (or their employers, in the case of works made for hire) the following rights:

(b)The right to post and update his or her Work on any internet site (other than the Author(s') personal web home page) provided that the following conditions are met: (i) access to the server does not depend on payment for access, subscription or membership fees; and (ii) any such posting made or updated after acceptance of the Work for publication includes and prominently displays the correct bibliographic data and an OSA copyright notice (e.g. "© 2009 The Optical Society").

17th December 2010

http://hdl.handle.net/2440/59681

Fluorescence-based sensing with optical nanowires: a generalized model and experimental validation

Stephen C. Warren-Smith*, Shahraam Afshar V., and Tanya M. Monro

Centre of Expertise in Photonics, Institute for Photonics & Advanced Sensing, School of Chemistry & Physics, University of Adelaide, Adelaide, SA 5005, Australia
**stephen.warrensmith@adelaide.edu.au*

Abstract: A model for the fluorescence sensing properties of small-core high-refractive-index fibers (optical nanowires) is developed and compared quantitatively with experiment. For the first time, higher-order modes and loss factors relevant to optical nanowires are included, which allows the model to be compared effectively with experiment via the use of fluorophore filled suspended optical nanowires. Numerical results show that high-index materials are beneficial for fluorescence-based sensing. However, both numerical and experimental results show that the fluorescence signal is relatively insensitive to core size, except for low concentration sensing where nanoscale fiber cores are advantageous due to the increased evanescent field power.

©2010 Optical Society of America

OCIS codes: (060.2370) Fiber optics sensors; (060.4005) microstructured fibers; (300.2530) fluorescence, laser-induced.

References and links

1. J. B. Jensen, P. E. Hoiby, G. Emiliyanov, O. Bang, L. H. Pedersen, and A. Bjarklev, "Selective detection of antibodies in microstructured polymer optical fibers," Opt. Express **13**(15), 5883–5889 (2005).
2. T. Ritari, J. Tuominen, H. Ludvigsen, J. C. Petersen, T. Sørensen, T. P. Hansen, and H. R. Simonsen, "Gas sensing using air-guiding photonic bandgap fibers," Opt. Express **12**(17), 4080–4087 (2004).
3. F. M. Cox, A. Argyros, and M. C. J. Large, "Liquid-filled hollow core microstructured polymer optical fiber," Opt. Express **14**(9), 4135–4140 (2006).
4. J. M. Fini, "Microstructure fibres for optical sensing in gases and liquids," Meas. Sci. Technol. **15**(6), 1120–1128 (2004).
5. S. Smolka, M. Barth, and O. Benson, "Highly efficient fluorescence sensing with hollow core photonic crystal fibers," Opt. Express **15**(20), 12783–12791 (2007).
6. Y. Ruan, T. C. Foo, S. C. Warren-Smith, P. Hoffmann, R. C. Moore, H. Ebendorff-Heidepriem, and T. M. Monro, "Antibody immobilization within glass microstructured fibers: a route to sensitive and selective biosensors," Opt. Express **16**(22), 18514–18523 (2008).
7. S. Afshar 5th, S. C. Warren-Smith, and T. M. Monro, "Enhancement of fluorescence-based sensing using microstructured optical fibres," Opt. Express **15**(26), 17891–17901 (2007).
8. S. Afshar 5th, Y. Ruan, S. C. Warren-Smith, and T. M. Monro, "Enhanced fluorescence sensing using microstructured optical fibers: a comparison of forward and backward collection modes," Opt. Lett. **33**(13), 1473–1475 (2008).
9. S. C. Warren-Smith, S. Afshar, and T. M. Monro, "Theoretical study of liquid-immersed exposed-core microstructured optical fibers for sensing," Opt. Express **16**(12), 9034–9045 (2008).
10. Y. Zhu, H. Du, and R. Bise, "Design of solid-core microstructured optical fiber with steering-wheel air cladding for optimal evanescent-field sensing," Opt. Express **14**(8), 3541–3546 (2006).
11. Y. N. Zhu, R. T. Bise, J. Kanka, P. Peterka, and H. Du, "Fabrication and characterization of solid-core photonic crystal fiber with steering-wheel air-cladding for strong evanescent field overlap," Opt. Commun. **281**(1), 55–60 (2008).
12. J. Lou, L. Tong, and Z. Ye, "Modeling of silica nanowires for optical sensing," Opt. Express **13**(6), 2135–2140 (2005).
13. Y. L. Ruan, E. P. Schartner, H. Ebendorff-Heidepriem, P. Hoffmann, and T. M. Monro, "Detection of quantum-dot labelled proteins using soft glass microstructured optical fibers," Opt. Express **15**(26), 17819–17826 (2007).
14. T. G. Euser, J. S. Y. Chen, M. Scharrer, P. St. J. Russell, N. J. Farrer, and P. J. Sadler, "Quantitative broadband chemical sensing in air-suspended solid-core fibers," J. Appl. Phys. **103**(10), 103108 (2008).
15. A. S. Webb, F. Poletti, D. J. Richardson, and J. K. Sahu, "Suspended-core holey fiber for evanescent-field sensing," Opt. Eng. **46**(1), 10501–10503 (2007).

#124483 - $15.00 USD Received 19 Feb 2010; revised 11 Apr 2010; accepted 13 Apr 2010; published 21 Apr 2010
(C) 2010 OSA

16. L. M. Tong, R. R. Gattass, J. B. Ashcom, S. L. He, J. Y. Lou, M. Y. Shen, I. Maxwell, and E. Mazur, "Subwavelength-diameter silica wires for low-loss optical wave guiding," Nature **426**(6968), 816–819 (2003).
17. H. Ebendorff-Heidepriem, S. C. Warren-Smith, and T. M. Monro, "Suspended nanowires: fabrication, design and characterization of fibers with nanoscale cores," Opt. Express **17**(4), 2646–2657 (2009).
18. T. R. Glass, S. Lackie, and T. Hirschfeld, "Effect of numerical aperture on signal level in cylindrical wave-guide evanescent fluorosensors," Appl. Opt. **26**(11), 2181–2187 (1987).
19. H. P. Kao, N. Yang, and J. S. Schoeniger, "Enhancement of evanescent fluorescence from fiber-optic sensors by thin-film sol-gel coatings," J. Opt. Soc. Am. A **15**(8), 2163–2171 (1998).
20. D. Marcuse, "Launching light into fiber cores from sources located in the cladding," J. Lightwave Technol. **6**(8), 1273–1279 (1988).
21. D. Marcuse, "Excitation of parabolic-index fibers with incoherent sources," Bell Syst. Tech. J. **54**, 1507–1530 (1975).
22. C. O. Egalon, R. S. Rogowski, and A. C. Tai, "Excitation efficiency of an optical fiber core source," Opt. Eng. **31**(6), 1328–1331 (1992).
23. C. O. Egalon, and R. S. Rogowski, "Efficiency of core light injection from sources in the cladding - bulk distribution," Opt. Eng. **31**(4), 846–851 (1992).
24. C. O. Egalon, and R. S. Rogowski, "Theoretical-model for a thin cylindrical film optical fiber fluorosensor," Opt. Eng. **31**(2), 237–244 (1992).
25. A. W. Snyder, and J. D. Love, *Optical Waveguide Theory* (Chapman and Hall, 1983).
26. K. Okamoto, *Fundamentals of Optical Waveguides* (Academic Press, 2000).
27. P. J. Roberts, F. Couny, H. Sabert, B. J. Mangan, T. A. Birks, J. C. Knight, and P. S. Russell, "Loss in solid-core photonic crystal fibers due to interface roughness scattering," Opt. Express **13**(20), 7779–7793 (2005).
28. G. Y. Zhai, and L. M. Tong, "Roughness-induced radiation losses in optical micro or nanofibers," Opt. Express **15**(21), 13805–13816 (2007).
29. L. Tong, L. Hu, J. Zhang, J. Qiu, Q. Yang, J. Lou, Y. Shen, J. He, and Z. Ye, "Photonic nanowires directly drawn from bulk glasses," Opt. Express **14**(1), 82–87 (2006).
30. A. Bryant, S. Albin, C. O. Egalon, and R. S. Rogowski, "Changes in the amount of core light injection for fluorescent-clad optical-fiber due to variations in the fiber refractive-index and core radius - experimental results," J. Opt. Soc. Am. B **12**(5), 904–906 (1995).
31. S. Albin, A. L. Bryant, C. O. Egalon, and R. S. Rogowski, "Injection efficiency from a side-excited thin-film fluorescent cladding of a circular wave-guide," Opt. Eng. **33**(4), 1172–1175 (1994).
32. F. W. D. Rost, *Fluorescence Microscopy* (Cambridge University Press, 1992)
33. E. P. Schartner, R. T. White, S. C. Warren-Smith, and T. M. Monro, "Practical sensitive fluorescence sensing with microstructured fibres," Proc. SPIE **7503**, 75035X (2009).

1. Introduction

Fluorescence sensing is an important tool for a wide range of applications, particularly for biological sensing through the use of fluorescent labeling. It has long been realized that these fluorescence-based techniques can be incorporated into an optical fiber platform and, in particular, microstructured optical fibers (MOFs) offer advantages such as long interaction length, high sensitivity, and small volume requirements [1]. One important parameter for fiber sensing is the fraction of optical power that propagates externally to the fiber substrate and can thus be used to interact with an analyte. Several types of MOF allow for high power fractions such as band-gap fibers [2, 3], liquid-core fibers [4, 5], and small-core fibers [6–17]. In addition, small-core high-index fibers have been predicted to offer increased sensitivity due to the presence of high intensity evanescent fields adjacent to the core-cladding interface [7]. Here we concentrate on small-core fibers due to the considerable interest that has recently been shown in both fabricating and sensing with these fibers. They are generally fabricated either as free-standing optical nanowires or suspended-core designs, where core diameters have been fabricated as small as 50nm [16] and 400nm [17] respectively. Their relatively simple filling requirements, compared to selective filling designs, also make them an ideal candidate for both testing the theoretical results in this paper and for future sensing applications.

In addition to knowing the power fraction of a given fiber design, which indicates how much fluorescence can be excited, it is important to be able to predict the efficiency with which the fluorescence is captured by the guided mode(s) of the fiber. This can be calculated using ray tracing methods [18, 19], however, these are unsuitable for the single/few-moded fibers considered here. A modal approach was first developed by Marcuse [20, 21] for the case of a uniform cladding excitation (e.g. side excitation) and found that fluorescence capture increased with increasing V-number. This uniform excitation theory was later generalized for vectorial step-index fiber solutions and it was shown that, more specifically,

#124483 - $15.00 USD Received 19 Feb 2010; revised 11 Apr 2010; accepted 13 Apr 2010; published 21 Apr 2010
(C) 2010 OSA

capture is increased with increasing refractive index difference between the core and cladding [22–24]. However, these results did not consider the case of a core pumped fiber and did not include effects due to fiber loss or Beer's law absorption. These factors have subsequently been included for the case of a suspended-core geometry (sometimes described as a wagon wheel or steering wheel), which have similar characteristics to conventional step-index fibers [7–9]. It was found that the existence of localized high-intensity electric and magnetic field layers of the fundamental mode at the boundary interface of small-core fibers leads to an increase in fluorescence capture when high index glasses are used.

In this paper the previous theoretical results [7–9] are extended to include the capture by higher order modes and to include additional loss mechanisms (confinement loss and small-core loss), which have not previously been incorporated into the theory. Combining these factors provides a rigorous model of the fluorescence sensing properties of optical nanowires, which we demonstrate is in quantitative agreement with experiment. In Sec. 2 we first describe the equations used for this numerical modeling. The fluorescence capture is then modeled, with higher order modes included, for parameters corresponding to MOFs that have recently been fabricated. To add confidence to the model numerical results are then compared with the ray optics equivalent and agreement is found in the regime of high V-number. Effects due to fluorophore absorption, confinement loss, and experimentally measured small-core loss are then included in the model. In Sec. 3 experimental results are compared with the numerical results of Sec. 2, which show quantitative agreement and also experimentally highlight which fiber parameters are best suited for low-concentration fluorescence-based sensing.

2. Numerical results

2.1 Fluorescence capture theory

The following equations (Eqs. 1(a), 1(b), and 1(c)) for the fluorescence capture are based on the derivation presented in [7]; the primary difference being that we retain the summation in Eq. 1(a) in order to include the contribution of higher order modes and thus extend our analysis to fibers that have core diameters outside of the single-mode regime. Also, additional loss mechanisms, which are implicit in the equations below, are included in Sec. 2.5.

To begin we assume that the fluorescent sources are contained within a cross sectional region *H* and that they have random phase and orientation [20]. *H* often refers to the fiber cladding (or holes), but can be any region that fluorescent sources are present, such as the centre of the core as will be considered in Sec. 2.2. Taking into account fiber loss and Beer's law absorption along the length of the fiber, the fraction of fluorescence (FCF) that is excited by excitation mode *j*, captured into all guided modes *v* of the fiber at the fluorescence wavelength, and propagates to the output end of a fiber can be expressed as [7]:

$$FCF_j = \frac{\xi\lambda^2}{16\pi n_F^{H\,2}} \sum_v \frac{NOI_{jv}}{A_{eff,v}} \frac{\gamma_j^H e^{-\gamma_v L}}{\gamma_v - \gamma_j} \left[e^{(\gamma_v - \gamma_j)L} - 1 \right] \tag{1a}$$

$$NOI_{jv} = n_F^H \left(\frac{\varepsilon_0}{\mu_0} \right)^{1/2} \left[\frac{\int_{A_\infty} |\, s_v(\vec{r}) \,| \, dA}{\int_H s_j(\vec{r}) dA} \right] \left[\frac{\int_H |\, \vec{e}_v \,|^2 s_j(\vec{r}) dA}{\int_{A_\infty} |\, s_v(\vec{r}) \,|^2 \, dA} \right] \tag{1b}$$

$$A_{eff,v} = \frac{|\int_{A_\infty} s_v(\vec{r}) dA \,|^2}{\int_{A_\infty} |\, s_v(\vec{r}) \,|^2 \, dA} \tag{1c}$$

#124483 - $15.00 USD Received 19 Feb 2010; revised 11 Apr 2010; accepted 13 Apr 2010; published 21 Apr 2010
(C) 2010 OSA

where A_∞ is defined to be the infinite transverse cross section, L is the fiber length, $s_j(\boldsymbol{r})$ is the z-component of the Poynting vector of the j^{th} mode, $\boldsymbol{e}_j(\boldsymbol{r})$ is the electric field of the j^{th} mode, λ is the fluorescence wavelength, ξ is the fluorophore efficiency, n_F^H is the refractive index in the region H at the fluorescence wavelength, *NOI* is a normalized overlap integral [7], A_{eff} is the modal effective area, and γ is the attenuation coefficient [25]. A similar expression can be found for fluorescence that propagates to the launch end of the fiber [8].

Equation (1) can be considered as consisting of two components, one longitudinal and the other transverse. The longitudinal component is contained within Eq. 1(a), which arises from considering the fibre attenuation at both excitation and fluorescence wavelengths, Beer's law absorption, and integration along the entire length of the fibre. The transverse component is primarily contained within Eqs. 1(b) and 1(c), where the effective area has been separated to give more physical insight into the fluorescence capture mechanism. It shows that the capture into a particular mode is proportional to how tightly that mode is confined.

2.2 Comparison between wave-optics and ray-optics approach

As the refractive index contrast is increased, the fiber becomes increasingly multi-mode and ray-tracing methods become applicable. Hence, the theory of Eq. (1) can be checked by testing convergence in the limit of increasing the number of modes. This is an important check as there are several assumptions that are associated with Eq. (1) [7] and because of the possibility of numerical errors as multiple integrations are required, particularly for highly multimode fibers. To perform the comparison we have taken the simple case of a fluorophore centered at the fiber axis (that is, in the core), and have calculated the fluorescence capture for the ideal case of a lossless step-index fiber. The step-index model with fully analytical vectorial solutions was used to determine the electric and magnetic fields [26]. The cladding refractive index was held constant at n = 1.0 and the core index varied from 1.01 to 11. For each curve the core radius was varied such that the V- number (thus number of modes) was held fixed, where $V = (2\pi a / \lambda)(n_{co}^2 - n_{cl}^2)^{1/2}$, a is the core radius, n_{co} is the core index, and n_{cl} is the cladding index [25]. Curves were then calculated with the V-number varying from 1.0 to 50. Several of these curves are displayed in Fig. 1 and are compared with the ray-tracing equivalent, which is defined as the fraction of fluorescence that is emitted within the critical angle of the fiber. This is written as $\frac{1}{2}(1-\cos(\theta_c))$, where θ_c is the fiber's critical angle.

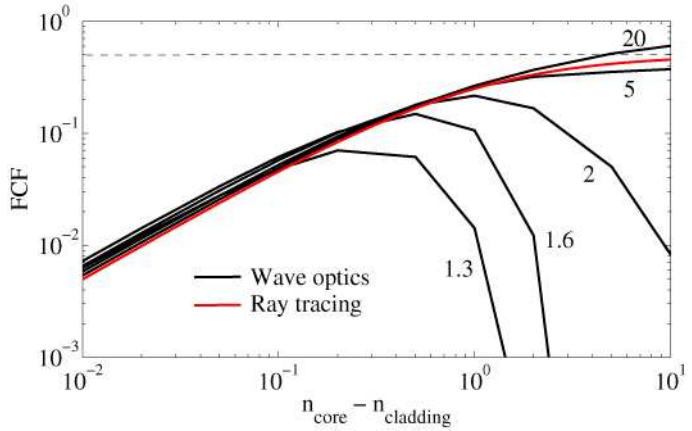

Fig. 1. Comparison of the wave-optics derived fluorescence capture fraction (FCF) for an on-axis in-core fluorophore (black) and the ray-tracing equivalent (red). The optical fiber V-number used for the wave-optics method is displayed in the figure for each corresponding curve. FCF = 0.5 (i.e. 50% capture) has been marked with a dashed line.

Figure 1 shows that the two rather different approaches agree remarkably well for sufficiently high V-number (V > 5), and also display the expected behavior. Firstly, both

#124483 - $15.00 USD Received 19 Feb 2010; revised 11 Apr 2010; accepted 13 Apr 2010; published 21 Apr 2010
(C) 2010 OSA

demonstrate that the fluorescence capture is dependent on the numerical aperture of the fiber. Also, for very large index differences, the fluorescence capture appears to asymptote below 50%, which is required for energy conservation (with a 50% maximum possible in either forwards or backwards directions). We see that for low V-numbers, particularly where the fiber is single-moded ($V < 2.405$), the two approaches yield differing results. Hence, we see that ray-optics is not a suitable model for studying the fluorescence capture behavior of single/few-moded fibers. To demonstrate the convergence of the two models as the V-number (and hence the number of modes) is increased, the fluorescence capture has been shown for two values of Δn in Fig. 2(a) (Δn = 0.01) and Fig. 2(b) (Δn = 1.0).

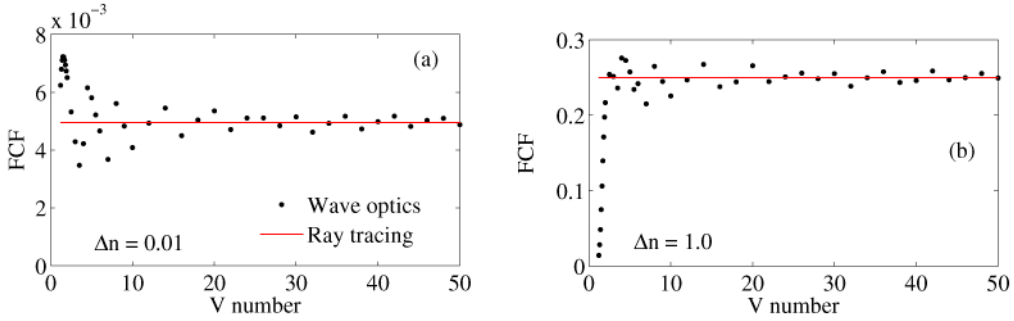

Fig. 2. Convergence of the wave-optics approach to the ray-optics approach for increasing optical fiber V-number. The difference in refractive index between the core and cladding (Δn) is 0.01 (a) and 1.0 (b).

Figure 2 shows that as the V-number is increased the two models converge to the same value. The close agreement between the two methods adds confidence to the theory of Eq. (1) and thus the following results presented in this paper.

2.3 Fluorescence capture

The fluorescence capture was then calculated for the case of a step-index fiber with a glass core and a water cladding. This is equivalent to considering an optical nanowire immersed in an aqueous analyte or approximately equivalent to a suspended-core fiber filled with an aqueous analyte. Several glass types with differing refractive index (silica ≈ 1.46, lead silicate (F2) ≈ 1.62, and bismuth ≈ 2.09) were considered for the core material, with an excitation wavelength of 532 nm and a single fluorescence wavelength of 590 nm (for example, rhodamine B dissolved in water). Unless otherwise specified, these values have been used in the remainder of this paper. To begin, the loss of the fiber was taken to be zero and the length to be infinite. In this way, the calculated FCF represents the fundamental limit on the fluorescence capture possible for the sensor design. Also, we have only used the fundamental mode to construct the excitation field, which is more or less accurate depending on the initial launch conditions. All guided modes of the fiber are excited to some degree by the fluorescence, and the results for the capture fraction summed across all of these modes are shown in Fig. 3(b).

#124483 - $15.00 USD Received 19 Feb 2010; revised 11 Apr 2010; accepted 13 Apr 2010; published 21 Apr 2010
(C) 2010 OSA

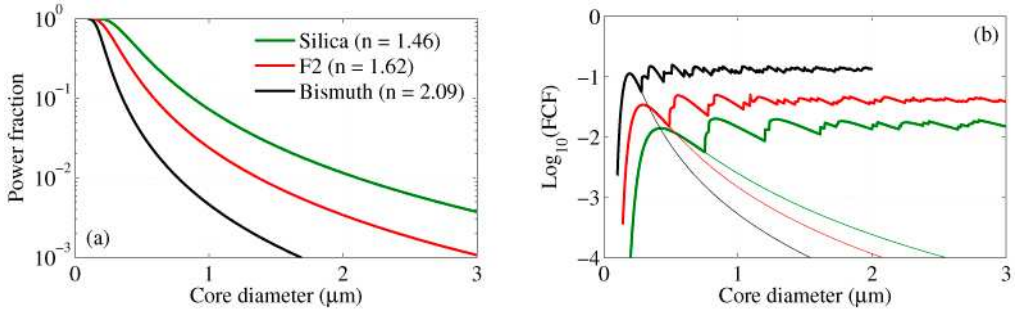

Fig. 3. (a) Fraction of fundamental mode evanescent field power located in the water for water-clad step-index fibers made from three different glass types. (b) Fluorescence capture into the fundamental mode only (thin lines) and into all guided modes (thick lines) for three different glasses where the cladding is Rhodamine B dissolved in water.

We see from Fig. 3(b) that the fluorescence capture is greatest for fibers whose core-cladding refractive index is greatest, regardless of the core diameter. That is, the result previously shown for side-excited fibers holds for core-pumped fibers [23]. This can be understood intuitively, that is, greater capture is, unsurprisingly, observed for fibers with larger numerical aperture. Additionally, we see that fluorescence capture into the fundamental mode only represents a significant portion of the overall capture for very small core diameter fibers (<< 1 micron). For core diameters larger than the single-mode regime, the fluorescence capture is achieved mostly through the higher order modes. In fact, we see that the contribution of the higher order modes is such that the fluorescence capture efficiency becomes insensitive to core diameter as the core diameter, and thus the number of modes, is increased. Note that the sharp peaks in the curves of Fig. 1(b) correspond to capture into higher order modes near cut-off. When confinement loss is considered, these peaks are smoothed, as will be discussed in Sec 2.5.

2.4 Fluorophore absorption

While the results of Fig. 3(b) show that the fluorescence capture efficiency is relatively insensitive to the core diameter, they do not consider the effect of absorption of the pump light along the length of the fiber, which depends on the fraction of power outside the core (Fig. 3(a)) as well as the chemical absorption coefficient. Assuming fundamental mode excitation, for a finite length fiber (1 m) and with varying concentrations of rhodamine B, the predicted backscattered fluorescence capture is shown in Fig. 4(a) for silica fibers and Fig. 4(b) for bismuth fibers. These calculations assume that the fiber material itself contributes no loss.

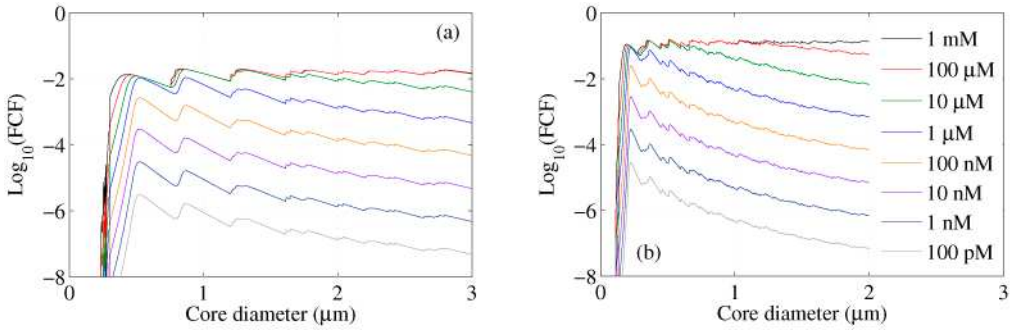

Fig. 4. Back scattered fluorescence signal for a silica fiber (a) and bismuth fiber (b) of length 1m, where the cladding contains varying concentrations of Rhodamine B.

Here we see that for high concentration solutions (e.g. > 100 μM, red and black curves), there is little core diameter dependence. This is because the excitation light is efficiently

#124483 - $15.00 USD Received 19 Feb 2010; revised 11 Apr 2010; accepted 13 Apr 2010; published 21 Apr 2010
(C) 2010 OSA

absorbed by the fluorophore for all core diameters despite differences in the power fraction. In contrast, when lower concentrations are used the excitation light is less efficiently absorbed for larger core diameter fibers due to the lower power fraction (Fig. 3(a)), resulting in a fluorescence signal that is dependent on core diameter. In fact, the optimum core diameter (silica = 540 nm and bismuth = 240 nm), which corresponds to the peak in the fundamental mode fluorescence capture, is up to 22 times larger for silica fibers and 360 times larger for bismuth fibers compared with a 2 μm core diameter fiber (for a 1 m fiber measuring 100 pM rhodamine B). Comparing silica fibers to bismuth fibers for low concentration sensing (1 nM) we see that at the optimum core diameter bismuth fibers can provide a factor of 9 times better fluorescence capture than silica fibers. This reduces to only 44% (bismuth compared to silica) when considering a core diameter of 2 μm due to a lower power fraction. Hence, to take advantage of higher fluorescence capture using high index fibers, small core diameters need to be used.

2.5 Confinement loss and small-core loss

The results of Fig. 4 indicate that the best fluorescence signal occurs for single-mode fibers with extremely small core diameters, such as 240 nm for a bismuth fiber. In reality there are several factors that prevent this from being the optimum choice. Inherent surface roughness at the core-cladding boundary is believed to be the major contribution to loss in small-core fibers and optical nanowires [27, 28]. Experimental measurements of small-core loss have previously been compiled [17], and these results have been used here to understand the effect on optimum core diameter. In addition, suspended-core fibers have an additional loss (confinement loss) due to the presence of an outer cladding with the same refractive index as the core material. While confinement loss can be reduced by increasing the separation between the core and the fiber jacket, in practice this becomes increasingly difficult as the core size decreases relative to the wavelength of the guided light.

The confinement loss was calculated by analytically determining the dispersion equation of a jacketed air suspended rod (JASR), which is a specific example of the well known W-fiber geometry, using a method analogous to the methods used for step-index fibers [26]. First, the wave equation was solved for the core, inner cladding, and outer cladding regions of the JASR by writing the electric and magnetic fields as appropriate superpositions of Bessel functions. Continuity of the tangential components of the electric and magnetic fields at the two boundaries was then imposed to create a dispersion relation by which the complex effective index was determined using *fsolve* from Matlab's optimization toolbox. The confinement loss (in dB/m) was then determined from the imaginary component of the effective index, n_i, using $\alpha_{dB} = 20\log_{10}(e)2\pi n_i / \lambda$. Results were obtained for the same parameters used in previous sections, including both excitation and fluorescence wavelengths. The results for the fluorescence wavelength are shown in Fig. 5(a) (silica), Fig. 5(b) (F2), and Fig. 5(c) (bismuth). Here the ratio of the outer cladding radius to the core radius was set at 10, which is close to that of recently fabricated suspended optical nanowires [17].

#124483 - $15.00 USD Received 19 Feb 2010; revised 11 Apr 2010; accepted 13 Apr 2010; published 21 Apr 2010
(C) 2010 OSA

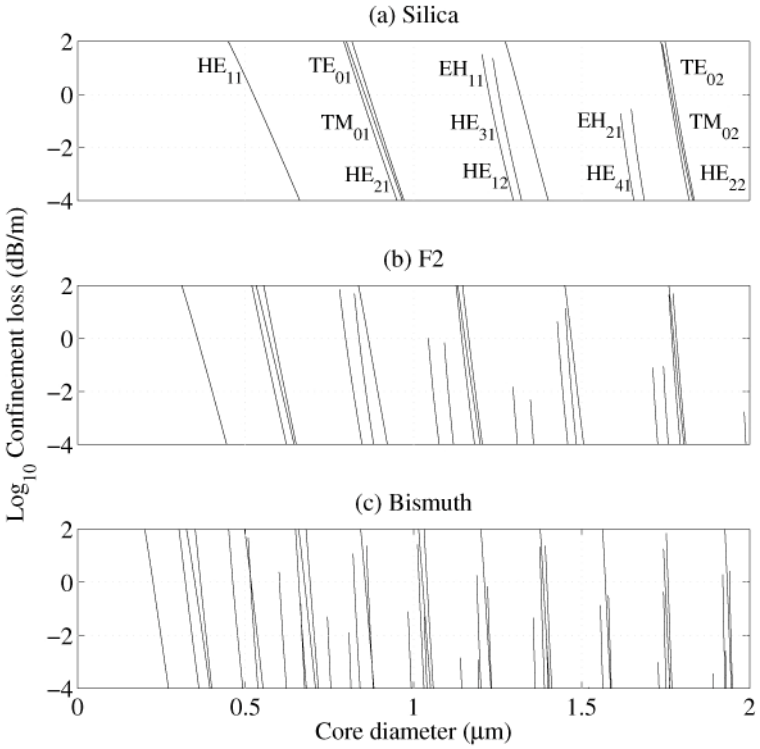

Fig. 5. Confinement loss of a W-fiber with a cladding to core ratio of 10, a wavelength of 590nm, and glass material silica (a), F2 (b), and bismuth (c). Mode labeling is shown for the silica material (a). The mode labeling is similar for F2 and bismuth but has not been displayed for clarity.

The results show a very steep increase in confinement loss as core diameter is reduced, which is steeper for higher order modes and higher index glasses. Note that they show there is only a restricted range of core diameters for which the fiber is effectively single mode. For example, if one requires a confinement loss of greater than 10 dB/m for the higher order modes in order to have effective single mode guidance, then the maximum core diameter for a single mode F2 nanowire only increases from 490 nm (for strict single mode guidance) to 540 nm (for effective single mode guidance).

To see the effect confinement loss has on the optimum core diameter for fluorescence sensing, Eq. (1) was again calculated but with the confinement loss at both excitation and fluorescence wavelengths included within the attenuation terms for a fiber of 1 m in length (Fig. 6). For clarity, the effect of fluorophore absorption was not included in these results, but will be included when comparing with experimental results in Sec. 3.

#124483 - $15.00 USD Received 19 Feb 2010; revised 11 Apr 2010; accepted 13 Apr 2010; published 21 Apr 2010
(C) 2010 OSA

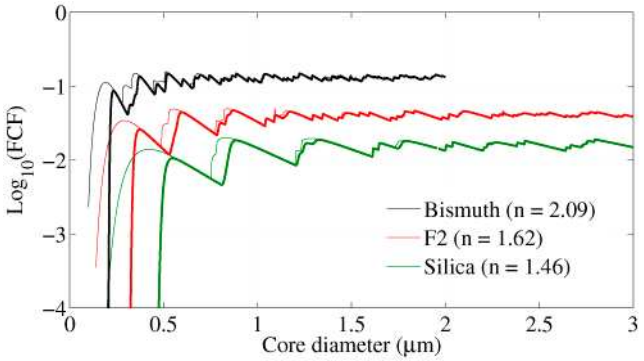

Fig. 6. Fluorescence capture into all modes of a step-index fiber with core material bismuth (black), F2 (red), and silica (green). The results of Fig. 3(b) have been shown again for the case of no confinement loss (thin lines), and then confinement loss has been included at both excitation and fluorescence wavelengths (thick lines). The fiber length has been set at 1 m, with fluorescence measured in the forward direction.

By comparing the thin lines (no confinement loss) and thick lines (confinement loss) in Fig. 6 we see that confinement loss has the effect of reducing the fluorescence capture peaks observed for the low mode number core diameters, as well as increasing the smallest core diameter fibers that can be used in practice. For example, the minimum core diameter, defined as the core diameter at which the capture is 0.1% ($\log_{10}$(FCF) = −3), increases from 90 nm to 210 nm for bismuth fibers, 150 nm to 330 nm for F2 fibers, and 230 nm to 490 nm for silica fibers. It also has the effect of smoothing the curves, as the sharp peaks observed in Fig. 3(b) were the result of capture into higher order modes near cut-off, at which point they are in reality rather lossy.

The next factor we include is experimentally measured small-core loss (Fig. 7). Experimental data for silicate fibers is shown in Fig. 7(a) [17, 29], and the line of best fit has been used to estimate the expected loss for a small-core lead-silicate (F2) fiber. Implicit is the assumption that the loss of the first silicate glass in Fig. 7(a) (Corning 0215, black data points) has similar properties to F2 glass. As with the confinement loss, the small-core loss was factored into the attenuation term of Eq. (1). The results are shown in Fig. 7(b) for an example case of a 1m long fiber with fluorescence captured in the forward direction, where confinement loss has been included for both, but fluorophore absorption effects (Fig. 4) neglected.

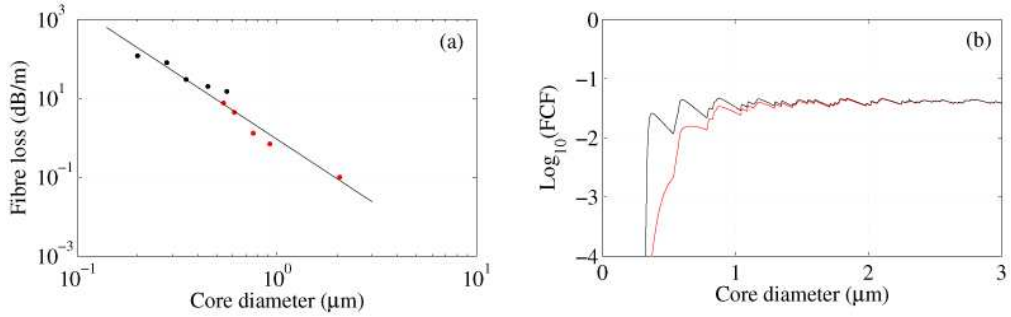

Fig. 7. (a) Measured loss at 633nm for small-core silicate tapers [29] (Corning 0215, n = 1.52, black data points) and F2 suspended-core fibers [17] (F2 Schott glass, n = 1.62, red data points). (b) Forwards fluorescence capture fraction for a 1 m F2 fiber with small-core loss considered (red) or small-core loss neglected (black). Confinement loss has also been included for both.

Figure 7(b) shows that small-core loss has a profound effect on fluorescence capture in the regime of subwavelength core diameters, dominating the impact of the confinement loss.

#124483 - $15.00 USD Received 19 Feb 2010; revised 11 Apr 2010; accepted 13 Apr 2010; published 21 Apr 2010
(C) 2010 OSA

Indeed, fluorescence capture into the fundamental mode is almost completely lost for a fiber only one meter long, implying that single-mode, and potentially few-moded, optical nanowires are not well suited to fluorescence capture for lengths the order of one meter or more. The next step is to combine the individual effects of fluorescence capture (Fig. 3), fluorophore absorption (Fig. 4), confinement loss (Fig. 6), and small-core loss (Fig. 7). These will now be combined for a specific example and compared with experimental results.

3. Experimental results

Only a modest amount of experimental work quantifying the behavior of optical fiber fluorescence sensors has been reported in the literature. Several authors have demonstrated that the fluorescence capture is proportional to the fiber's numerical aperture [18, 30, 31]. Bryant *et al* demonstrated that the signal level obtained from thin-film side-excited fiber increases with increasing core diameter [30]. Afshar *et al* also confirmed several predictions in regards to the length dependence of an optical fiber fluorescence sensor [8], such as the presence of an optimum length when measured in the forwards direction and no optimum length for the backwards direction. For the first time, we present here experimental results that are quantitatively compared with fluorescence capture theory for small-core fibers. We compare the experimental results with predictions made in Sec. 2, in regards to the dependence of fluorescence signal on core diameter and fluorophore concentration.

To perform these experiments, a number of F2 (lead-silicate Schott glass) suspended-core fibers where fabricated with a range of core diameters (620 nm, 770 nm, 920 nm, 1290 nm, 2050 nm) [17]. These fibers were cleaved to 26 cm lengths and filled with various concentrations of Rhodamine B dissolved in water. Prior to filling, excitation light (532 nm) was launched into the fiber core and the output power was recorded to determine the coupling efficiency. After filling, the forward fluorescence signal was measured after passing through one or two 550 nm long pass filters. The measured data was corrected for the power loss due to the quantum efficiency of the Rhodamine B (70%) and the long pass filter(s) (66-89%, depending on filter used). Also, an optical spectrum analyzer (ANDO AQ6315E) was used for low concentration samples due to the need to filter out the pump light, for these the data was multiplied by 11.1 to take into account the spectral bandwidth of the fluorescence spectrum that was recorded (585 to 595 nm out of a rhodamine spectrum that ranges from approximately 520 nm to 700 nm, measured using a rhodamine B sample in a cuvette). Additionally, for the two highest concentration samples, fluorescence re-absorption was estimated using theory and was factored into the measured data (factor of up to 3.5). These experimental results are shown in Fig. 8 on the same scale as the equivalent theoretical results. The theoretical curves include all effects that were considered in Sec. 2; fluorescence capture, fluorophore absorption, confinement loss, and core-size dependent surface roughness loss. Note that no free parameters have been used.

#124483 - $15.00 USD Received 19 Feb 2010; revised 11 Apr 2010; accepted 13 Apr 2010; published 21 Apr 2010
(C) 2010 OSA

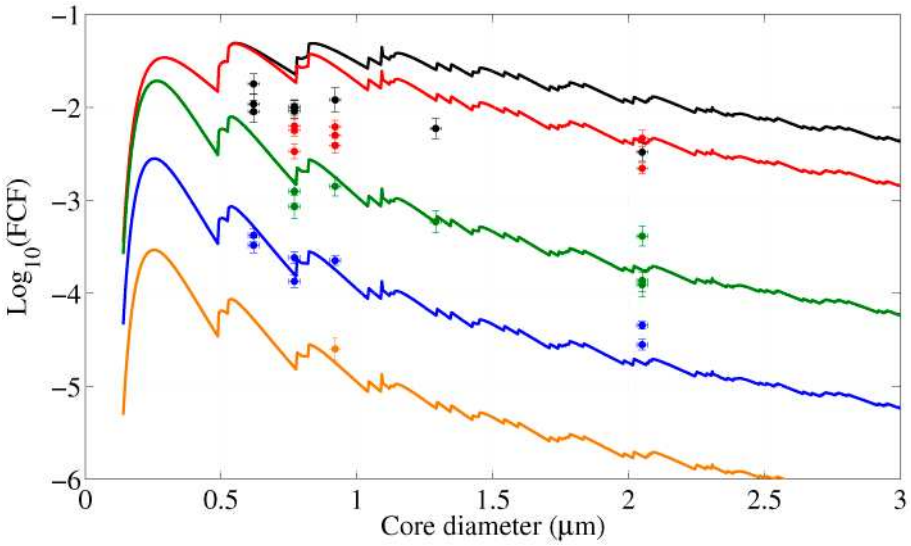

Fig. 8. Predicted forward fluorescence signal for 0.26 m long F2 step-index fibers (solid lines) and measured signal for equivalent suspended-core fibers (data points). For the predicted curves small-core loss and confinement loss has been included. The excitation wavelength was 532 nm and fluorescence wavelength for the theory was 590 nm. The rhodamine B concentrations were 50 μM (black), 25 μM (red), 1 μM (green), 100 nM (blue), and 10 nM (orange). The vertical error bars refer to signal fluctuation during measurement (≈10 s), and horizontal error bars relative to SEM resolution.

The experimental results compare well quantitatively with theory, particularly for low concentration samples. For higher concentration samples (≥ 25 μM), the measured results were found to be lower than expected, and reasons for this may include concentration quenching [32], or stronger than estimated reabsorption. Also, the lower concentration measurements (≤ 1 μM) for the 2.05 μm fiber appear to be higher than that predicted by theory. This could indicate the presence of multimode excitation light, which could be considered in future theoretical work.

The experimental results confirm several important points. Firstly, in the limit of high concentration samples the dependence on core diameter is quite small. This is due to near-complete pump absorption even at large core diameters. In contrast, stronger signals are obtained from smaller core fibers when low concentration samples are used, with up to an order of magnitude difference observed between 620 nm and 2050 nm core diameter fibers.

4. Conclusions

The fluorescence sensing properties of core-pumped high-refractive-index optical nanowires have been explored theoretically and experimentally. Evanescently excited fluorescence is most efficiently captured into fibers made from high refractive index materials due to their relatively high numerical aperture. We also predict that there is very little dependence on core diameter when considering only the fluorescence capture, due to the role of higher order modes, which have been taken into account in the model for the first time here. However, when also considering the Beer's law absorption of the excitation light the higher power fraction of small core fibers can provide a stronger fluorescence signal, particularly for low concentration sensing. We then include loss effects that are characteristic for optical nanowires, such as confinement loss and experimentally measured loss arising from surface-roughness. These effects dictate the minimum core diameter fiber that can be efficiently used for sensing. For example, a 1-meter long F2 optical nanowire would not be useful if the core diameter is less than approximately 400 nm. These results thus set a guideline for future fiber fabrication for optimal sensor design.

#124483 - $15.00 USD Received 19 Feb 2010; revised 11 Apr 2010; accepted 13 Apr 2010; published 21 Apr 2010
(C) 2010 OSA

Of course, these results are specific to the parameters considered here and would vary for, say, different fluorophores, fluorophore concentrations, fiber lengths, and fiber substrates. For example, if only very short lengths of fiber were to be used, then the minimum useful core diameter would be reduced. Other factors, such as coupling efficiency and stability, could also be included in future analysis. In particular, coupling stability into sub-micron core optical nanowires needs careful attention before these devices are to become practical.

Our experimental results using F2 suspended-core fibers are in close agreement with the numerical results. Notably, both the theoretical and experimental results show that the advantage of using small-core fibers (e.g. 620 nm compared to 2 μm) is most significant for low concentration sensing (< 1 μM for the example in this paper); where up to an order of magnitude improvement can be obtained. The experimental results show successful fluorescence measurement for a fluorophore (rhodamine B in this case) with a concentration as low as 10 nM. While it was not the aim of this paper to present detection of extremely low concentrations, lower concentrations could be measured by using detector sources with lower noise, longer interaction lengths, and moving to higher index optical fibers. Indeed, it has been shown previously that 200 pM detection is possible using similar fibers [33].

In summary, we have presented a rigorous model for predicting the fluorescence sensing performance of optical nanowires, which is in agreement with experimental results. The model is a useful tool for the optimization of optical nanowire sensing designs and the numerical results highlight the benefits of small-core high-refractive-index optical nanowires, particularly for low concentration sensing.

Acknowledgments

We acknowledge the support of the Defence Science and Technology Organisation (DSTO), Australia, and in particular the DSTO Corporate Initiative on Smart Materials and Structures for sponsorship of this program of research. We acknowledge the Australian Research Council for funding this project (DP0880436). T. Monro acknowledges the support of an Australian Research Council Federation Fellowship. We acknowledge Heike Ebendorff-Heidepriem and Roger Moore for fiber fabrication.

#124483 - $15.00 USD Received 19 Feb 2010; revised 11 Apr 2010; accepted 13 Apr 2010; published 21 Apr 2010
(C) 2010 OSA